

Cite this: *Energy Environ. Sci.*,  
2022, 15, 4015

## Determining overpotentials for the oxidation of alcohols by molecular electrocatalysts in non-aqueous solvents†

Amy L. Speelman,<sup>a</sup> James B. Gerken,<sup>b</sup> Spencer P. Heins,<sup>a</sup> Eric S. Wiedner,<sup>a</sup> Shannon S. Stahl<sup>b</sup> and Aaron M. Appel<sup>b\*</sup>

Molecular electrocatalysts for energy-related transformations offer unique opportunities to elucidate mechanistic principles that contribute to improved rates and energy efficiency. New catalysts for electrochemical alcohol oxidation in non-aqueous conditions have been developed recently, but it is difficult to make meaningful performance comparisons between them because the different conditions used for each catalyst result in unquantified differences in driving force. The present report outlines an approach to determine the equilibrium potential for the oxidation of alcohols in organic solvents or solvent mixtures. These equilibrium potentials are then used to determine the overpotentials for a series of molecular electrocatalysts. Overall, the methodology outlined herein provides a foundation for future advances in this field and enables comparison of electrocatalyst performance under aqueous and non-aqueous reaction conditions.

Received 6th May 2022,  
Accepted 9th August 2022

DOI: 10.1039/d2ee01458k

rsc.li/ees

### Broader context

Electrocatalytic alcohol oxidation is a key process in direct methanol fuel cells and is the focus of growing attention in biomass conversion and electrochemical synthesis. Significant effort has therefore been directed toward the design of molecular electrocatalysts for alcohol oxidation. Reactions with these catalysts are often performed in non-aqueous solvents and under different reaction conditions, which complicates quantitative comparisons of catalyst performance and thereby impedes progress in this field. This perspective outlines an approach to assess overpotentials for catalytic reactions under any conditions, enabling meaningful comparison of different catalysts and providing a foundation to establish criteria for the design of new catalytic systems.

## Introduction

Alcohol oxidation is a fundamental functional group transformation that is of interest in both synthetic and energy-related contexts. As an anode reaction in fuel cells, it is imperative that oxidation takes place at an electrode potential close to the thermodynamic potential of the reaction. Although this is less critical in the context of synthetic alcohol oxidation, the energetic requirements for a process can impact reaction selectivity and, potentially, economic viability. Thus, it is important to know not only the operating potential of an alcohol oxidation catalyst, but also how that potential is related to the

thermodynamic potential of the overall reaction under the catalytic conditions.

Overpotential ( $\eta$ ) is generally defined as the difference between the equilibrium potential of the reaction being catalyzed and the potential at which a catalyst operates at a specific current.<sup>1</sup> In other words, overpotential is an indicator of the excess electrochemical driving force for catalysis at a given rate. It is therefore essential to report the electrocatalytic rate and the corresponding overpotential together since each can be improved at the cost of the other.

To determine an overpotential, both the catalytic potential and equilibrium potential must be well-defined. For molecular electrocatalysts, the catalytic wave typically occurs near a redox couple of the parent complex and reaches a steady-state current ( $i_{\text{cat}}$ ) at sufficiently anodic potentials (or cathodic potentials, for reduction reactions). The selection of a catalytic potential can be somewhat subjective because similar values of  $i_{\text{cat}}$  are observed over a range of potentials. The overpotential of a molecular catalyst is therefore frequently reported at the

<sup>a</sup> Center for Molecular Electrocatalysis, Pacific Northwest National Laboratory, Richland, WA 99352, USA. E-mail: aaron.appel@pnnl.gov

<sup>b</sup> Department of Chemistry, University of Wisconsin–Madison, Madison, Wisconsin 53706-1322, USA

† Electronic supplementary information (ESI) available. See DOI: <https://doi.org/10.1039/d2ee01458k>



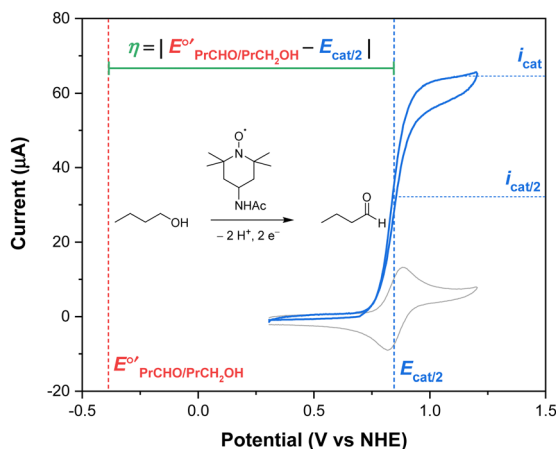


Fig. 1 Overpotential is the difference between the thermodynamic potential ( $E_{\text{RCHO/RCH}_2\text{OH}}^\circ$ ) and the potential for catalysis ( $E_{\text{cat}/2}$ ), as illustrated for the oxidation of 1-butanol to butanal catalyzed by ACT in water at pH 10. Data from ref. 3.

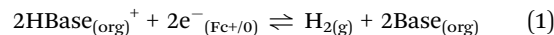
catalytic half-wave potential ( $E_{\text{cat}/2}$ ), defined as the potential at which the current of the catalytic wave reaches half of  $i_{\text{cat}}$ .<sup>1,2</sup> This concept is illustrated in Fig. 1 for the electrocatalytic oxidation of 1-butanol to butanal using 4-acetamido-TEMPO (ACT, TEMPO = 2,2,6,6-tetramethylpiperidine-*N*-oxyl).<sup>3</sup> By using this approach, the current and potential are well-defined and coupled to each other. The equilibrium potential for a catalytic reaction ( $E^\circ$ ) is determined from the standard potential ( $E^\circ$ ) by accounting for non-standard state reaction conditions, specifically for temperatures other than 298 K and any reactant or product that does not have a solution concentration of 1 M (or 1 atm for gases). Buffering is recommended any time an overpotential is determined in order to provide a stable, well-defined thermodynamic potential, but is particularly important when the overpotential is low.<sup>1</sup>

The ability to accurately define the thermodynamic potential for a reaction under each set of catalytic conditions is crucial to enable meaningful comparisons of overpotentials with different catalysts. Direct experimental measurement of  $E^\circ$  requires an electrode that can reversibly and rapidly perform the electrochemical reaction of interest. In cases like alcohol oxidation where no such electrode exists,  $E^\circ$  may be calculated from the free energies of formation of the substrate(s) and product(s). Using this method, the standard potentials of many redox reactions have been reported in aqueous solution.<sup>4</sup> However, molecular electrocatalysts are often studied in organic solvents or solvent mixtures in which standard potentials are not known.

In this manuscript, we report a method for determining the thermodynamic potentials for the oxidation of alcohols under non-aqueous conditions, including the  $2e^-/2H^+$  interconversion of several common aldehydes and ketones with the corresponding alcohol, the  $4e^-/4H^+$  oxidations of primary alcohols to esters and carboxylic acids, and the  $6e^-/6H^+$  oxidation of methanol to  $\text{CO}_2$ . These potentials allow, for the first time, a direct quantification of the overpotential for alcohol oxidation with molecular electrocatalysts in organic solvents.

## Calculation of standard potentials for the oxidation of alcohols

A crucial advance in evaluating overpotentials in organic solvents and solvent mixtures came with the application of open-circuit potential (OCP) measurements for the direct determination of the equilibrium potentials for the hydrogen evolution reaction (eqn (1)) in organic solvents, measured vs. the ferrocenium/ferrocene ( $\text{Fc}^{+/0}$ ) couple ( $E_{\text{BH}^+/\text{H}_2(\text{org})}$ ).<sup>5</sup>



In this method,  $E_{\text{BH}^+/\text{H}_2(\text{org})}$  is determined by measuring the OCP of buffered mixtures of an acid and its conjugate base under 1 atm  $\text{H}_2$  using a Pt electrode freshly annealed in a  $\text{H}_2$  flame. In solvents with an established absolute  $\text{pK}_a$  scale, the OCP method can also be used to determine the standard hydrogen couple ( $E_{\text{H}^+/\text{H}_2(\text{org})}^\circ$ ) via eqn (2).

$$E_{\text{H}^+/\text{H}_2(\text{org})}^\circ = E_{\text{BH}^+/\text{H}_2(\text{org})} + 0.0592 * \text{pK}_a(\text{org}) \quad (2)$$

Using this approach, values of  $E_{\text{H}^+/\text{H}_2}^\circ$  have been reported in several solvents (see Table S3, ESI†), including MeCN ( $E_{\text{H}^+/\text{H}_2(\text{MeCN})}^\circ = -0.028 \text{ V vs. Fc}^{+/0}$ ).<sup>5</sup> We note that the value reported in THF ( $E_{\text{H}^+/\text{H}_2(\text{THF})}^\circ = -0.343 \text{ V vs. Fc}^{+/0}$ ) was calculated using an absolute  $\text{pK}_a$  scale<sup>7</sup> which is different from the most commonly used  $\text{pK}_a$  scale in THF (sometimes referred to the  $\text{pK}_a$  scale).<sup>8</sup> Although only a few absolute  $\text{pK}_a$  values have been directly determined,  $\text{pK}_a$  values, which have been reported for a wide variety of bases, can be used to calculate approximate  $\text{pK}_a$  values (see ESI,† Section 2a for a more detailed discussion).

Based on  $E_{\text{BH}^+/\text{H}_2(\text{org})}$ , thermochemical cycles can be constructed to determine the thermodynamic potentials for reactions involving transfer of  $\text{H}_2$  equivalents. This approach has been previously used to establish standard potentials for reduction of gaseous small molecules ( $\text{O}_2$ ,  $\text{CO}_2$ , and  $\text{N}_2$ ) in organic solvents<sup>9,10</sup> as well as for oxidation of a limited number of alcohols in water or MeCN.<sup>11–13</sup>

A thermochemical cycle for determination of standard potentials for 2-electron oxidation of alcohols ( $E_{\text{R}_2\text{CO}/\text{R}_2\text{CHOH}(\text{org})}^\circ$ ) is shown in Fig. 2.<sup>14</sup> The cycle starts from  $E_{\text{H}^+/\text{H}_2(\text{org})}^\circ$  and the gas-phase free energy for aldehyde or ketone hydrogenation ( $\Delta G_{+\text{H}_2(\text{g})}^\circ$ ), which can be calculated from the difference in the gas-phase free energies of formation ( $\Delta G_{\text{f}(\text{g})}^\circ$ ) of the pure aldehyde or ketone and alcohol. It also involves the difference in solvation free energy between the alcohol and aldehyde or ketone ( $\Delta\Delta G_{\text{solv}}^\circ$ ). Although solvation free energies for common alcohols, aldehydes, and ketones are known in aqueous solution, few have been reported in the organic solvents commonly used in electrochemical studies of alcohol oxidation. However, since an alcohol and the corresponding aldehyde or ketone have nearly identical sizes and only modest differences in polarity,  $\Delta\Delta G_{\text{solv}}^\circ$  is likely to be a relatively small contributor to the potential. In support of this assumption, the contributions of solvation free energy terms to the aqueous standard potentials for the oxidation of ethanol, 2-propanol, and



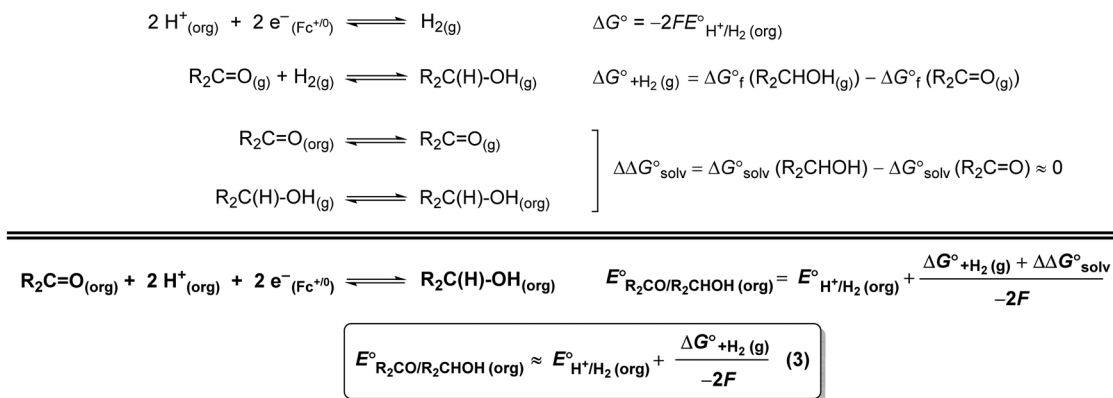


Fig. 2 By combining the potential of the  $\text{H}^+/\text{H}_2$  couple and the free energy for hydrogenation of an aldehyde or ketone, the standard potentials for 2-electron oxidation of alcohols have been estimated in organic solvents.

benzyl alcohol are between 20 and 50 mV (see ESI† Section 4a for the complete analysis). In the solvents typically used in electrochemical experiments with organometallic and inorganic complexes, the magnitude of  $\Delta \Delta G^\circ_{\text{solv}}$  is likely to be similar to or smaller than the value in water (see ESI† Section 4b). Based on its very limited contribution to the potential,  $\Delta \Delta G^\circ_{\text{solv}}$  can be omitted when solvation free energies are not available. In these cases,  $E^\circ_{\text{R}_2\text{CO}/\text{R}_2\text{CHOH}(\text{org})}$  is calculated using eqn (3), shown at the bottom of Fig. 2. Values of  $E^\circ_{\text{R}_2\text{CO}/\text{R}_2\text{CHOH}(\text{org})}$  in water, MeCN, and THF are provided in Table 1 for several common alcohols.

The same approach can be used for the 4  $\text{e}^-$  oxidation of alcohols to esters or carboxylic acids (see ESI† Sections 5 and 6 for complete analysis).<sup>16</sup> We note that there is a greater degree of uncertainty in the values for carboxylic acids and carboxylates because in organic solvents these species are prone to aggregation, including homoconjugation, dimerization, and ion pairing, which perturbs solution equilibria and changes

the driving force for the overall reaction. The impact of aggregation can be included if all of the relevant equilibrium constants are known. When they are not known, the influence of aggregation can be minimized by conducting measurements of  $E_{\text{cat}/2}$  in buffered solutions containing the acid, base, alcohol, and carboxylic acid.<sup>1</sup>

An analogous thermochemical scheme for determination of the standard potential for the 6  $\text{e}^-$  oxidation of methanol to  $\text{CO}_2$  is discussed in the ESI† (Section 7). Because  $\text{CO}_2$  has a gas-phase standard state, a correction for its solvation free energy is not included. The solvation free energy term for the alcohol therefore makes a slightly larger contribution to the potential compared to the 2-electron and 4-electron cases. When solvation free energies are not available, a better estimate of  $E^\circ_{\text{CO}_2/\text{MeOH}(\text{org})}$  can be obtained based on  $E^\circ_{\text{CO}_2/\text{MeOH}(\text{aq})}$  (see ESI,† Section 7c) following the approach described in ref. 9.

Table 1 Standard potentials for oxidation of alcohols calculated using the approach in Fig. 2. The aqueous values include a solvation free energy correction, and the non-aqueous values were calculated assuming  $\Delta \Delta G^\circ_{\text{solv}} = 0$ , except where noted

Reaction	Alcohol	$E^\circ_{\text{product}/\text{alcohol}(\text{solvent})}$		
		Water (V vs. SHE)	MeCN (V vs. $\text{Fc}^{+/0}$ )	THF (V vs. $\text{Fc}^{+/0}$ )
$\text{R}_2\text{CO}_{(\text{solv})} + 2\text{H}_{(\text{solv})}^+ + 2\text{e}^- \rightleftharpoons \text{R}_2\text{CHOH}_{(\text{solv})}$	MeOH	0.23 <sup>a</sup>	0.28 <sup>b</sup>	−0.03 <sup>b</sup>
	EtOH	0.21	0.15	−0.16
	<sup>t</sup> PrOH	0.13	0.08	−0.24
	BnOH	0.18	0.10	−0.21
$\text{RC}(\text{O})\text{OCH}_2\text{R}_{(\text{solv})} + 4\text{H}_{(\text{solv})}^+ + 4\text{e}^- \rightleftharpoons 2\text{RCH}_2\text{OH}_{(\text{solv})}$	MeOH	—	0.04	−0.28
	EtOH	—	0.01 <sup>c</sup>	−0.33
$\text{RCO}_2\text{H}_{(\text{solv})} + 4\text{H}_{(\text{solv})}^+ + 4\text{e}^- \rightleftharpoons \text{RCH}_2\text{OH}_{(\text{solv})} + \text{H}_2\text{O}_{(\text{solv})}$ <sup>d</sup>	MeOH	0.11	0.08	−0.24
	EtOH	0.06	0.04 <sup>c</sup>	−0.29
	BnOH	0.06	0.03	−0.28
$\text{CO}_{2(\text{g})} + 6\text{H}_{(\text{solv})}^+ + 6\text{e}^- \rightleftharpoons \text{MeOH}_{(\text{solv})} + \text{H}_2\text{O}_{(\text{solv})}$	MeOH	0.03	0.00 <sup>c</sup>	−0.31 <sup>c</sup>

<sup>a</sup> Literature value for oxidation of methanol to methanediol.<sup>15</sup> See ESI Section 4a for further discussion. <sup>b</sup> These values correspond to the standard potential for the oxidation of methanol to formaldehyde. As discussed in more detail in ESI Section 4a, significant additional driving force for methanol oxidation is likely provided by condensation and oligomerization. Values calculated using this standard potential therefore correspond to a lower limit on the overpotential. <sup>c</sup> Values were calculated including an estimate for  $\Delta \Delta G^\circ_{\text{solv}}$ . See ESI Sections 5, 6, and 7 for more details.

<sup>d</sup> Under basic conditions where  $\text{p}K_{\text{a}}(\text{HBase}^+) > \text{p}K_{\text{a}}(\text{RCO}_2\text{H})$ , the thermodynamic potential for the carboxylate/alcohol pair is calculated as  $E^\circ_{\text{RCO}_2^-/\text{RCH}_2\text{OH}} = E^\circ_{\text{RCO}_2\text{H}} + 0.015 * \text{p}K_{\text{a}}(\text{RCO}_2\text{H}) - 0.074 * \text{p}K_{\text{a}}(\text{HBase}^+)$ . See ESI Section 6 for complete analysis.



We note that the thermodynamic potentials calculated using the above schemes involve several approximations. In addition to neglecting the contribution from solvation free energies, the analysis described above assumes ideal solutions (*i.e.*, that the activities of all species are equal to their nominal concentrations). While the impacts on the thermodynamic potentials are expected to be small, the resulting overpotentials, particularly when they are low, should be interpreted with these sources of uncertainty in mind.

### Calculation of equilibrium potentials under catalytic conditions

The values of  $E^\circ$  discussed above correspond to standard-state conditions of 1 M solvated  $H^+$ , 1 M alcohol, and 1 M oxidized product at 298 K. Electrochemical experiments are rarely performed under standard-state conditions, however, and it is necessary to determine the equilibrium potential ( $E^{\circ'}$ ) under the conditions employed in the experiment. The following discussion explains how to calculate  $E^{\circ'}$  for 2  $e^-$  oxidation of alcohols. The same approach may be used for 4  $e^-$  and 6  $e^-$  oxidations of alcohols.

Under non-aqueous conditions, alcohol oxidation is generally conducted in the presence of an organic base. In solvents with an established  $pK_a$  scale, the value of  $E^{\circ'}$  can be calculated from  $E^\circ$  and the  $pK_a$  of the protonated form of the organic base using eqn (4), shown at the bottom of Fig. 3. In solvents or solvent mixtures in which a  $pK_a$  scale has not been established or  $E_{H^+/H_2(ORG)}$  is not known,  $E^{\circ'}$  can instead be calculated from  $E_{BH^+/H_2(ORG)}$  (determined *via* OCP measurements using the same acid/base pair employed in the catalytic conditions) and  $\Delta G_{+H_2(g)}^\circ$  (see ESI,† Section 2b).

The analysis in Fig. 3 indicates that the choice of base has a substantial impact on the value of  $E_{R_2CO/R_2CHOH(ORG)}^{\circ'}$ . Fig. 4 shows the range of thermodynamic potentials for bases that have been used in reports of electrocatalytic oxidation of benzyl alcohol in MeCN and 2-propanol in THF. Use of the organic bases triethylamine ( $NEt_3$ ) and *N*-methyl imidazole (NMI) in MeCN, rather than standard-state conditions (*i.e.*, solvated  $H^+$ ), results in an  $\sim 1$  V shift in the thermodynamic potential for the PhCHO/BnOH redox equilibrium. Studies in THF have used even stronger phosphazene bases, leading to shifts of up to 2.2 V from standard-state potentials.

Electrocatalytic measurements are also often performed on solutions containing only alcohol and base. Under these

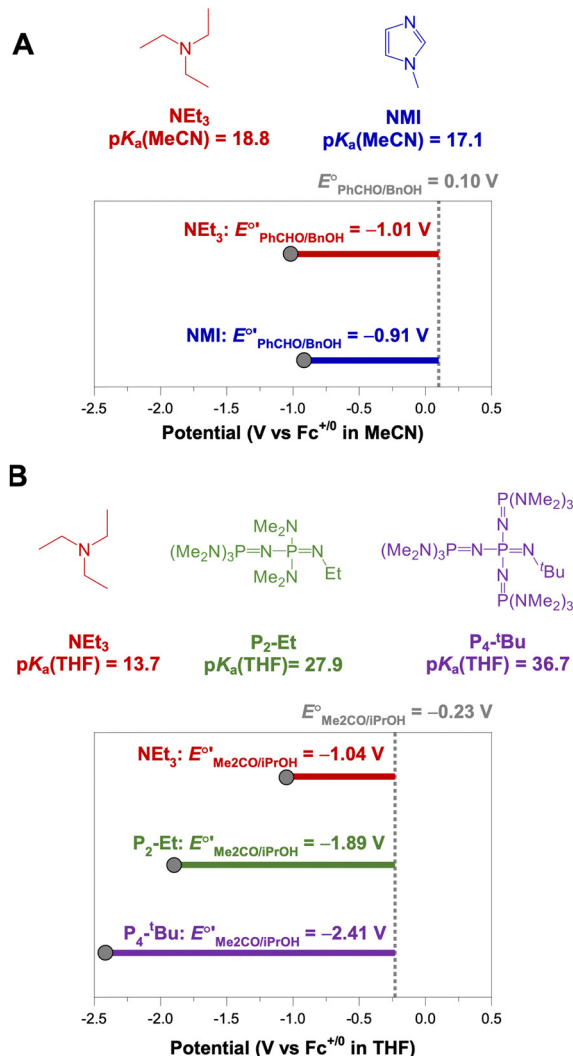


Fig. 4 Calculation of  $E^{\circ'}$  for 2-electron oxidation of benzyl alcohol in MeCN (A) and 2-electron oxidation of 2-propanol to acetone in THF (B) with different bases from the standard potential (see Table 1) and  $pK_a(H\text{-Base}^+)$  using eqn (4).

conditions, the thermodynamic potential is ill-defined because the  $\ln(Q)$  term in the Nernst equation contains terms with initial values of zero. Therefore, the solution composition at the electrode surface, and the corresponding electrode potential, change substantially as soon as electrocatalysis begins. If the measurement is instead performed using a buffered solution (containing a base, its conjugate acid, an alcohol, and the

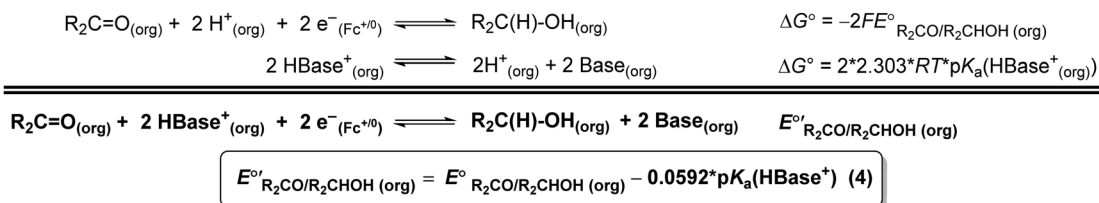


Fig. 3 Calculation of the thermodynamic potential for 2  $e^-$  oxidation of an alcohol in the presence of an acid/base pair ( $E^{\circ'}$  from  $E^\circ_{R_2CO/R_2CHOH(ORG)}$  and  $pK_a(H\text{-Base}^+)$  (see Fig. 2) and  $pK_a(H\text{-Base}^+)$ ).



corresponding aldehyde or ketone), the relative change in  $\ln(Q)$  and correspondingly in the thermodynamic potential will be small. The most straightforward method for establishing a stable potential is to perform electrocatalytic reactions in solutions containing 1:1 ratios of base to conjugate acid and alcohol to conjugate aldehyde or ketone. The resulting potential is the same as that calculated from eqn (4), despite the deviation from standard state conditions. If ratios other than 1:1 are used,  $E_{R_2CO/R_2CHOH(org)}^{o'}$  must be modified *via* the Nernst equation (eqn (5)) to account for the non-standard state concentrations.

$$E_{R_2CO/R_2CHOH(org)}^{o'} = E_{R_2CO/R_2CHOH(org)}^o - 0.0592 * \text{p}K_a(\text{HBase}^+) - \frac{RT}{2F} \ln\left(\frac{[\text{R}_2\text{CHOH}][\text{Base}]^2}{[\text{R}_2\text{C}=\text{O}][\text{HBase}^+]^2}\right) \quad (5)$$

### Evaluation of overpotential for known electrocatalysts for oxidation of alcohols

Molecular catalysts for electrochemical alcohol oxidation have been reviewed recently.<sup>17–19</sup> Here, we focus on a subset of catalysts for which electrochemical two-electron oxidation of alcohols was performed in THF or MeCN using bases with known  $\text{p}K_a$  values, which allows the determination of overpotentials (Fig. 5 and Table 2).

As discussed in the previous section, catalyst performance should be evaluated under buffered conditions. Such conditions are rarely employed in practice, and it is difficult to accurately predict what impact buffering will have on the observed catalytic rate and potential. To illustrate the impact of buffering, the oxidations of BnOH and <sup>i</sup>PrOH catalyzed by  $[\text{Ni}(\text{P}_2^{\text{tBu}}\text{N}_2^{\text{tBu}})(\text{MeCN})_2]^{2+}$  ( $\text{MeCN})_2][\text{BF}_4]_2$  were examined under unbuffered conditions

(only alcohol and  $\text{Et}_3\text{N}$ ) and buffered conditions (alcohol, PhCHO or  $\text{Me}_2\text{CO}$ ,  $\text{Et}_3\text{N}$ , and  $\text{Et}_3\text{NH}^+$ ). As shown in Fig. S7 and S8 (ESI<sup>†</sup>), for this specific catalyst buffering results in a small ( $\sim 50$  mV) positive shift in  $E_{\text{cat}/2}$  and an approximately two-fold decrease in rate. The precise changes will not be generalizable across catalysts, but this example shows that measuring under buffered conditions can result in a change in catalytic performance in some cases. This approach has not been used for the other systems in Fig. 5; the reported performance for these catalysts should be interpreted with this discrepancy in mind, especially for the values in THF that are expected to be more significantly impacted by the effects of ion pairing. To illustrate how the catalyst properties contribute to both overpotential and rate, the proposed catalytic cycles for several of these systems are discussed in detail below.

Under the buffered conditions described above,  $[\text{Ni}(\text{P}_2^{\text{tBu}}\text{N}_2^{\text{tBu}})(\text{MeCN})_2]^{2+}$  catalyzes the oxidation of BnOH at  $E_{\text{cat}/2} = -0.71$  V vs.  $\text{Fc}^{+/0}$ , corresponding to an overpotential of 0.39 V. As shown in Fig. 6, the catalytic cycle is proposed to involve generation of an alkoxide complex as the rate-limiting step.<sup>21</sup> This species undergoes  $\beta$ -hydride elimination to release benzaldehyde. Oxidation of the resulting Ni(II) hydride, which is the potential determining step, occurs at a mild potential because of the presence of the pendant amine, which provides a pathway for intramolecular proton transfer.<sup>29,30</sup> Although the Ni(II) hydride could not be isolated, this hypothesis is supported by comparison to related bis(diphosphine) Ni(II)–H complexes. For example, the oxidation of  $[\text{HNi}(\text{depp})_2]^+$  (depp = 1,3-bis(diethylphosphino)propane) occurs 0.6 V more positive than the oxidation of a corresponding complex that contains a pendant amine ( $[\text{HNi}(\text{Et}_2\text{PCH}_2\text{NMeCH}_2\text{PET}_2)_2]^+$ ).<sup>31</sup> The presence of the pendant amine is therefore crucial to achieving a low overpotential in this system. An analogous catalytic cycle was proposed for  $[\text{Co}(\text{P}_3)(\text{MeCN})_2]^{2+}$ , but the Co(II)–H is oxidized at a

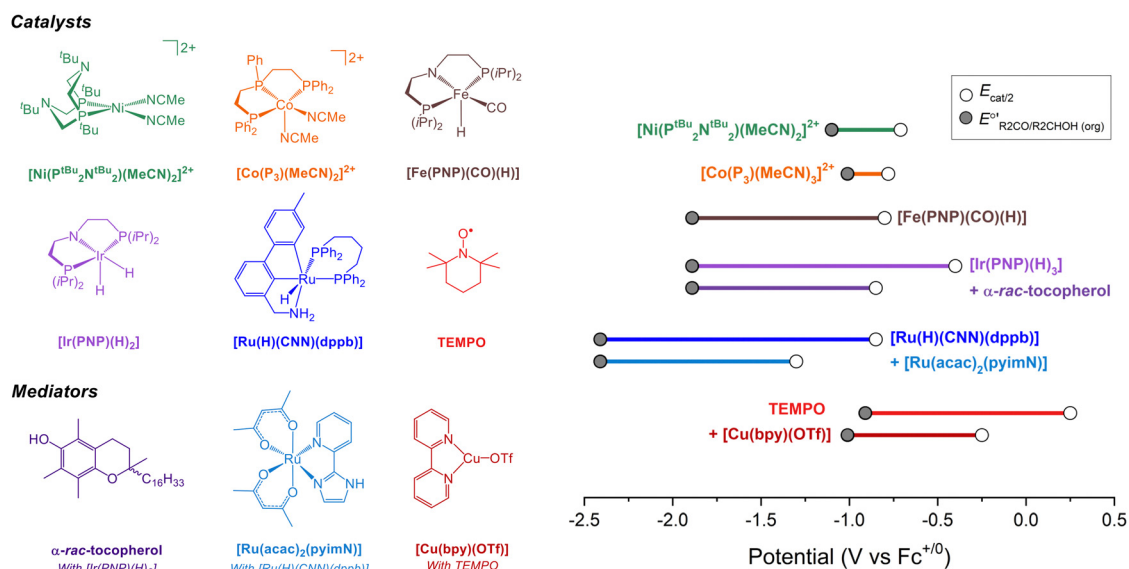


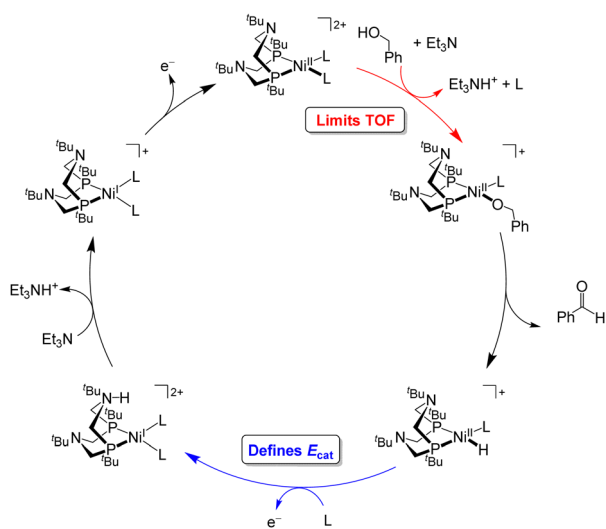
Fig. 5 (Left) Molecular catalysts for oxidation of alcohols in organic solution. (Right) Illustration of the overpotentials for oxidation of alcohols by molecular catalysts. The grey circles represent  $E_{R_2CO/R_2CHOH(org)}^{o'}$  (see Fig. 4) and the white circles represent  $E_{\text{cat}/2}$ . The length of the colored bars corresponds to the overpotential (see also Table 2).



Table 2 Overpotentials and catalytic rates for oxidation of alcohols by molecular electrocatalysts

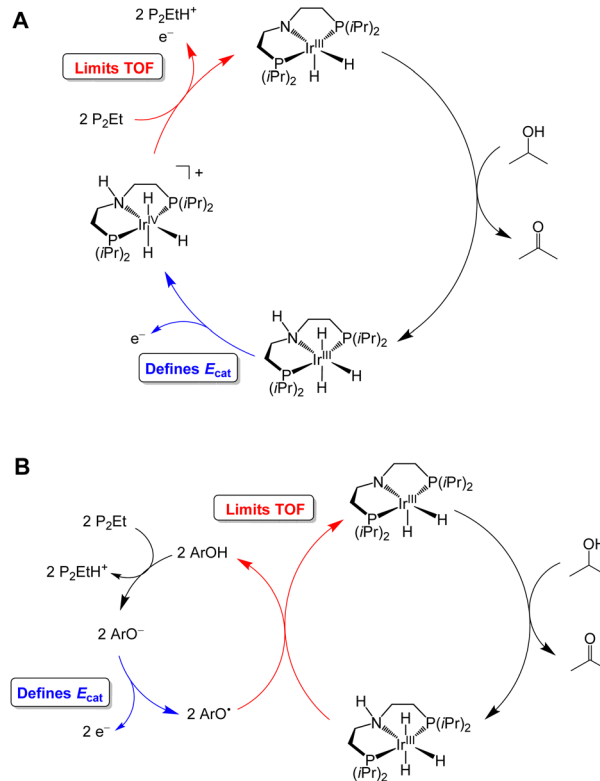
Catalyst	Solvent	ROH	Base (pK <sub>a</sub> ) <sup>a</sup>	η (V)	k <sub>obs</sub> (s <sup>-1</sup> )	Ref.
[Ni(P <sup>t</sup> Bu <sub>2</sub> N <sub>2</sub> <sup>t</sup> Bu)(MeCN) <sub>2</sub> ][BF <sub>4</sub> ] <sub>2</sub> <sup>b</sup>	MeCN	<sup>i</sup> PrOH	NEt <sub>3</sub> (18.8)	0.32 <sup>b</sup>	2.1	20 and 21
[Ni(P <sup>t</sup> Bu <sub>2</sub> N <sub>2</sub> <sup>t</sup> Bu)(MeCN) <sub>2</sub> ][BF <sub>4</sub> ] <sub>2</sub> <sup>b</sup>	MeCN	BnOH	NEt <sub>3</sub> (18.8)	0.39 <sup>b</sup>	4.5	20 and 21
[Co(P <sub>3</sub> )(MeCN) <sub>2</sub> ][BF <sub>4</sub> ] <sub>2</sub>	MeCN	BnOH	NEt <sub>3</sub> (18.8)	~0.2 <sup>c</sup>	<0.1 <sup>c</sup>	22
[Fe(PNP)(CO)(H)]	THF	<sup>i</sup> PrOH	P <sub>2</sub> -Et (27.9)	1.1 <sup>d</sup>	1.7	23
[Ir(PNP)(H) <sub>2</sub> ]	THF	<sup>i</sup> PrOH	P <sub>2</sub> -Et (27.9)	1.5 <sup>d</sup>	<i>n.d.</i> <sup>e</sup>	24
[Ir(PNP)(H) <sub>2</sub> ] with α-rac-tocopherol	THF	<sup>i</sup> PrOH	P <sub>2</sub> -Et (27.9)	1.0 <sup>d</sup>	14.6	24
[Ru(H)(CNN)(dppb)]	THF	<sup>i</sup> PrOH	P <sub>4</sub> <sup>t</sup> Bu (36.7)	1.6 <sup>d</sup>	0.6	25 and 26
[Ru(H)(CNN)(dppb)] with [Ru(acac) <sub>2</sub> (pyimN)]	THF	<sup>i</sup> PrOH	P <sub>4</sub> <sup>t</sup> Bu (36.7)	1.1 <sup>d</sup>	0.3	25 and 26
TEMPO	MeCN	BnOH	NMI (17.1)	1.2 <sup>d</sup>	2.3	27
TEMPO with [Cu(bpy)(OTf)]	MeCN	BnOH	NEt <sub>3</sub> (18.8)	0.8 <sup>d</sup>	11.6	27

<sup>a</sup> pK<sub>a</sub> refers to the conjugate acid of the indicated base. pK<sub>a</sub> values in MeCN were taken from the literature.<sup>8,28</sup> pK<sub>a</sub> values in THF<sup>8</sup> were converted<sup>7</sup> to absolute pK<sub>a</sub> values (see ESI section 2a). <sup>b</sup> Measurements were conducted on buffered solutions (see ESI Section 9). <sup>c</sup> No electrocatalytic activity was observed on the CV timescale, but bulk electrolysis at an applied potential of -0.63 V produced PhCHO with 97% Faradaic efficiency. η was estimated based on the Co(II/I) E<sub>1/2</sub> (-0.78 V vs. Fc<sup>+/0</sup>). <sup>d</sup> Measurements were not conducted under buffered conditions which increases the uncertainty in η. Values are therefore reported to the nearest 100 mV. <sup>e</sup> Rate not determined due to overlap of catalytic wave with background base oxidation by the electrode.

Fig. 6 Catalytic cycle for oxidation of benzyl alcohol by [Ni(P<sup>t</sup>Bu<sub>2</sub>N<sub>2</sub><sup>t</sup>Bu)(MeCN)<sub>2</sub>]<sup>2+</sup>.

mild potential without the need for a pendant amine.<sup>22</sup> This complex has a similar overpotential to [Ni(P<sup>t</sup>Bu<sub>2</sub>N<sub>2</sub><sup>t</sup>Bu)(MeCN)<sub>2</sub>]<sup>2+</sup> but a much lower catalytic rate.

Waymouth and co-workers have reported several electrocatalysts for the oxidation of 2-propanol based on thermal catalysts that were originally used for acceptorless alcohol dehydrogenation and transfer hydrogenation reactions.<sup>32–35</sup> The proposed catalytic cycle for [Ir(PNP)(H)<sub>2</sub>] is shown as a representative example in Fig. 7A. This complex dehydrogenates 2-propanol *via* a mechanism involving proton transfer to the PNP ligand amide group and hydride transfer to the Ir center to produce acetone and [Ir(PN(H)P)(H)<sub>3</sub>].<sup>24,35</sup> This species is oxidized at -0.65 V vs. Fc<sup>+/0</sup> and then deprotonated by phosphazene P<sub>2</sub>-Et. The strong base makes a large contribution to E<sup>cat</sup>, which results in a high overpotential of 1.5 V. Oxidation of 2-propanol by [Fe(PNP)(CO)(H)] follows an analogous mechanism.<sup>23</sup>

Fig. 7 Proposed catalytic cycle for oxidation of 2-propanol by [Ir(PNP)(H)<sub>2</sub>] in the absence (A) and presence (B) of a phenoxyl radical mediator.

Although the E<sub>cat/2</sub> is slightly more modest for the Fe complex, the use of a strong base (phosphazene P<sub>2</sub>-Et) results in a high overpotential of 1.1 V.

The overpotential of the Ir catalyst can be decreased by addition of a phenol/phenoxyl radical electron–proton transfer mediator,<sup>36</sup> which performs two successive formal H-atom abstractions to regenerate [Ir(PNP)(H)<sub>2</sub>] (Fig. 7B).<sup>24</sup> The mediator



is then regenerated electrochemically through deprotonation of the phenol by  $P_2$ -Et and oxidation of the phenoxide at  $-1.07$  V vs.  $Fe^{+/0}$ . Since this oxidation occurs at a milder potential than the oxidation of  $[Ir(PN(H)P)(H)_3]$ , the overpotential is decreased to 1.0 V. Similarly, the addition of  $[Ru(acac)_2(pyimN)]$  to  $[Ru(H)(CNN)(dppb)]$  lowers the overpotential for 2-propanol oxidation from 1.6 V to 1.1 V with phosphazene  $P_4$ - $t$ Bu as the base.<sup>25,26</sup> The origin of the decrease in overpotential is less clear in this case, but has been proposed to involve H-atom abstraction by  $[Ru(acac)_2(pyimN)]$ .

Organic aminoxyls, such as TEMPO and ACT, have been widely used as molecular electrocatalysts for alcohol oxidation.<sup>37</sup> As a representative example, the oxidation of benzyl alcohol occurs *via* reaction of the alcohol with  $TEMPO^+$  (Fig. 8A) to give TEMPOH and benzaldehyde.<sup>27,38</sup> TEMPOH is then deprotonated and re-oxidized to  $TEMPO^+$  at a potential of  $+0.24$  V vs.  $Fe^{+/0}$  in MeCN. The overpotential for this reaction is 1.2 V when NMI is used as the base. The addition of a Cu co-catalyst, which was originally developed to support aerobic alcohol oxidation,<sup>39</sup> has also been shown to enhance electrocatalytic alcohol oxidation. In this case,  $[Cu(bpy)]^{2+}$  and TEMPO mediate alcohol oxidation by a different mechanism in which the  $Cu^{II}$  and  $TEMPO^{\bullet}$  species act cooperatively to achieve net hydride abstraction from a Cu-coordinated alkoxide (Fig. 8B). Formation of the Cu-alkoxide complex is the rate-limiting step in this reaction. The  $[Cu(bpy)]^{2+}$  species also promotes proton-coupled oxidation of TEMPOH to regenerate  $TEMPO^{\bullet}$ ; oxidation of  $[Cu(bpy)]^+$  is the potential-determining step of the electrocatalytic reaction. This redox step

occurs at a more moderate potential than the oxidation of  $TEMPO^{\bullet}$  to  $TEMPO^+$ , resulting in a lower overpotential of 0.8 V.

### Comparison of overpotentials for the oxidation of alcohols

Using the approach described above, overpotentials for electrocatalytic alcohol oxidation can be meaningfully compared across solvents and conditions, as illustrated in Fig. 9A. Among the catalysts discussed so far,  $[Co(P_3)(MeCN)_2]^{2+}$  exhibits the lowest overpotential for alcohol oxidation, but it is significantly slower than the other catalysts.  $[Ni(P_2^{tBu}N_2^{tBu})(MeCN)_2]^{2+}$  also has a relatively low overpotential of 0.3–0.4 V while maintaining a similar rate to most of the catalysts. Other systems have  $\eta \geq 0.8$  V. Although mediators can be used to decrease the operating potential for 2-propanol oxidation by  $[Ir(PNP)(H)_2]$  and  $[Ru(H)(CNN)(dppb)]$ , the overpotentials remain high because strong bases are still used. Likewise, although the addition of  $[Cu(bpy)]^{2+}$  lowers  $E_{cat/2}$  for TEMPO-catalyzed BnOH oxidation, the overpotential remains high because a relatively high potential is still needed to oxidize  $[Cu(bpy)]^+$ .

The well-defined overpotentials discussed above for catalysts that operate in organic solvents also provide a basis for clearer comparison with catalysts operating under aqueous conditions. Fig. 9B shows examples of catalysts from different classes that operate in aqueous solution. TEMPO and its analogues catalyze the oxidation of a variety of alcohols in water, although the reactions generally occur at high overpotential. For example, the overpotential for ABNO-catalyzed oxidation of 1-butanol to

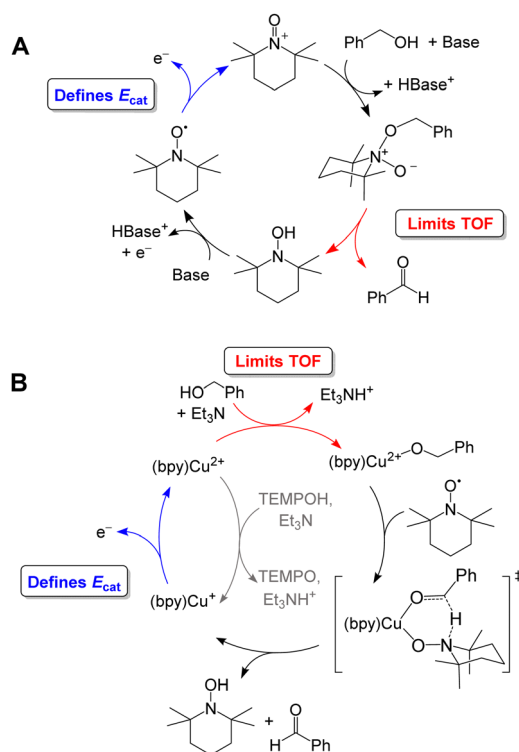


Fig. 8 Proposed catalytic cycle for oxidation of benzyl alcohol by TEMPO in the absence (A) and presence (B) of  $[Cu(bpy)]^{2+}$ .

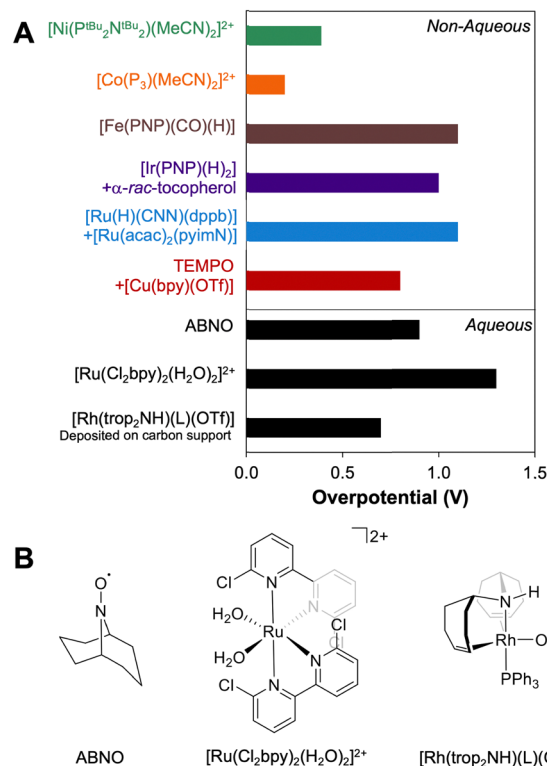


Fig. 9 (A) Comparison of the overpotentials for alcohol oxidation in organic solvents and under aqueous conditions. (B) Selected examples of electrocatalysts for oxidation of alcohols under aqueous conditions.



butanal is 0.9 V at pH 9.<sup>3</sup> By modifying the pH and the identity of the nitroxyl, the overpotential can be lowered by 0.15 V, but at a cost to the rate.<sup>40</sup> A variety of polypyridyl Ru complexes can also catalyze oxidation of alcohols, but generally require high overpotentials ( $\eta \geq 1$  V) because their mechanisms involve electrochemical generation of a Ru-oxo species at high potential.<sup>41–47</sup> As a representative example,  $[\text{Ru}(\text{Cl}_2\text{bpy})_2(\text{H}_2\text{O})_2]^{2+}$  catalyzes the 2-electron oxidations of methanol, ethanol, 2-propanol, and benzyl alcohol at pH 1.1 with overpotentials of 1.3–1.4 V.<sup>41</sup> Organometallic complexes immobilized on carbon supports have also been used for electrochemical alcohol oxidation under aqueous conditions.<sup>48–51</sup> For example,  $[\text{Rh}(\text{trop}_2\text{NH})(\text{PPh}_3)(\text{OTf})]$  catalyzes oxidation of ethanol to acetate with overpotentials  $> 0.7$  V at pH 12 when deposited on carbon black.<sup>50,51</sup>

For comparison, Pt/Ru alloys are among the most active heterogeneous catalysts for oxidation of alcohols and have been widely studied in direct methanol fuel cells.<sup>52–55</sup> Under the acidic conditions typical for proton-exchange membrane fuel cells, these alloys exhibit overpotentials as low as 0.3 V for conversion of MeOH to  $\text{CO}_2$ .<sup>53</sup> Unfortunately, these catalysts are poisoned by aldehydes and carboxylic acids, limiting their utility with alcohol substrates containing C–C bonds.<sup>54</sup> At high pH, metal oxides such as NiOOH have been used to promote electrocatalytic alcohol oxidation, and exhibit good activity, stability, and selectivity for oxidation of primary alcohols to carboxylates. However, these reactions require potentials approaching those capable of supporting water oxidation, resulting in overpotentials for alcohol oxidation of up to 1.3 V.<sup>56–59</sup>

## Conclusions

The methodology outlined herein provides an important foundation for future advances in the field of electrocatalytic alcohol oxidation by enabling comparisons of catalyst performance across different reaction conditions. Compared to previous studies in water, studies of reactivity and catalytic properties in organic solvents can be performed under a wider range of conditions. To date, overpotentials have not been reported for molecular electrocatalysts for the oxidation of alcohols in non-aqueous solvents because of the lack of established thermodynamic potentials, and this gap has hindered meaningful comparisons between catalysts studied under different conditions. The analysis above highlights the crucial role of both solvent and base strength on the thermodynamic potential of alcohol oxidation and shows how these two features combine with the electrochemical properties of the catalyst to establish the overpotential for electrocatalytic alcohol oxidation.

To summarize briefly, the overpotential for alcohol oxidation with a catalyst corresponds to the difference between the thermodynamic potential for the reaction under the conditions used for catalysis and the potential at which catalysis occurs at a given rate. Estimation of thermodynamic potentials for the 2  $e^-$ , 4  $e^-$ , and 6  $e^-$  oxidation of alcohols in organic solvents requires three values:

(1) The equilibrium potential for the hydrogen evolution reaction ( $E_{\text{BH}^+/\text{H}_2(\text{org})}$ ) in organic solvent with the acid-base pair used in the catalytic reaction.

(2) Values for the gas-phase free-energies of formation ( $\Delta G_f^\circ$ ) of the alcohol and oxidized product.

(3) An approximation for the difference in solvation free energies of the alcohol and oxidized product ( $\Delta\Delta G_{\text{solv}}^\circ$ ).

In solvents with an established  $\text{p}K_a$  scale,  $E_{\text{BH}^+/\text{H}_2(\text{org})}$  can be determined from  $E_{\text{H}^+/\text{H}_2(\text{org})}^\circ$  and  $\text{p}K_a(\text{HBase}^+)$ . OCP measurements can also be used to directly determine this benchmark value when there is no established  $\text{p}K_a$  scale for a solvent or  $E_{\text{H}^+/\text{H}_2(\text{org})}^\circ$  is not known. For the remaining two values,  $\Delta G_f^\circ$  is known for the common species of interest, and  $\Delta\Delta G_{\text{solv}}^\circ$  is expected to be small (*ca.* 1–2 kcal mol<sup>-1</sup>) based on known values for relevant species.<sup>60</sup> The resulting uncertainty ( $\lesssim 50$  mV) is often small relative to the operating overpotentials and  $\Delta\Delta G_{\text{solv}}^\circ$  can therefore be reasonably omitted in most cases.

The approach provided here has enabled comparison of the overpotentials for the oxidation of alcohols by molecular electrocatalysts in organic solvents. From this analysis,  $[\text{Ni}(\text{P}_2^{\text{Bu}}\text{N}_2^{\text{Bu}})(\text{MeCN})_2]^{2+}$  is noteworthy for its combination of good rate and comparatively low overpotential for catalysis. The lower overpotential is a result of a less positive potential for oxidation of the catalytically relevant species and the ability of the catalyst to operate with a modest base, resulting in a mild thermodynamic potential. As this field of research grows, the approach outlined here provides a basis for quantitative comparisons of catalyst performance, thereby facilitating the identification of catalyst properties that contribute to higher activities and lower overpotentials.

## Conflicts of interest

There are no conflicts to declare.

## Acknowledgements

This work was supported as part of the Center for Molecular Electrocatalysis, an Energy Frontier Research Center funded by the U.S. Department of Energy, Office of Science, Basic Energy Sciences.

## Notes and references

- 1 A. M. Appel and M. L. Helm, *ACS Catal.*, 2014, **4**, 630–633.
- 2 B. M. Stratakes, J. L. Dempsey and A. J. M. Miller, *Chem-ElectroChem*, 2021, **8**, 4161–4180.
- 3 M. Rafiee, K. C. Miles and S. S. Stahl, *J. Am. Chem. Soc.*, 2015, **137**, 14751–14757.
- 4 J. E. Nutting, J. B. Gerken, A. G. Stamoulis, D. L. Bruns and S. S. Stahl, *J. Org. Chem.*, 2021, **86**, 15875–15885.
- 5 J. A. Roberts and R. M. Bullock, *Inorg. Chem.*, 2013, **52**, 3823–3835.
- 6 R. G. Agarwal, S. C. Coste, B. D. Groff, A. M. Heuer, H. Noh, G. A. Parada, C. F. Wise, E. M. Nichols, J. J. Warren and J. M. Mayer, *Chem. Rev.*, 2022, **122**, 1–49.





- 7 G. Garrido, E. Koort, C. Rafols, E. Bosch, T. Rodima, I. Leito and M. Roses, *J. Org. Chem.*, 2006, **71**, 9062–9067.
- 8 S. Tshepelevitsh, A. Kütt, M. Lõkov, I. Kaljurand, J. Saame, A. Heering, P. G. Plieger, R. Vianello and I. Leito, *Eur. J. Org. Chem.*, 2019, 6735–6748.
- 9 M. L. Pegis, J. A. Roberts, D. J. Wasylenko, E. A. Mader, A. M. Appel and J. M. Mayer, *Inorg. Chem.*, 2015, **54**, 11883–11888.
- 10 B. M. Lindley, A. M. Appel, K. Krogh-Jespersen, J. M. Mayer and A. J. M. Miller, *ACS Energy Lett.*, 2016, **1**, 698–704.
- 11 Y. Wang, S. Gonell, U. R. Mathiyazhagan, Y. Liu, D. Wang, A. J. M. Miller and T. J. Meyer, *ACS Appl. Energy Mater.*, 2018, **2**, 97–101.
- 12 While this manuscript was in preparation, standard potentials in acetonitrile were reported (ref. 13) for a subset of the couples discussed in this manuscript. That work followed a similar approach to the one described here and the resulting values are within expected error of those reported here (see ESI† Section S8).
- 13 I. Fokin, K.-T. Kuessner and I. Siewert, *Synthesis*, 2021, 295–314.
- 14 Two alternative thermochemical cycles are discussed in ESI† Section S4c.
- 15 A. J. Bard, R. Parsons and J. Jordan, *Standard Potentials in Aqueous Solution*, Marcel Dekker, Inc., New York, 1985.
- 16 An alternative thermochemical scheme for calculation of  $E_{\text{HCO}_2\text{H}/\text{MeOH}}^\circ$  can also be constructed based on the hydricity of formate in acetonitrile (see ESI† Section S6d). This scheme requires  $E_{\text{CO}_2/\text{MeOH}}^\circ$  in acetonitrile, but avoids the requirement for the solvation free energy of formic acid in acetonitrile. The  $E_{\text{HCO}_2\text{H}/\text{MeOH}}^\circ$  calculated from this cycle is identical to the value calculated from  $\Delta G_{+2\text{H}_2}^\circ$ .
- 17 A. W. Cook and K. M. Waldie, *ACS Appl. Energy Mater.*, 2019, **3**, 38–46.
- 18 N. Wolff, O. Rivada-Wheellaghan and D. Tocqueville, *Chem-ElectroChem*, 2021, **8**, 4019–4027.
- 19 M. Bellini, M. Bevilacqua, A. Marchionni, H. A. Miller, J. Filippi, H. Grützmacher and F. Vizza, *Eur. J. Inorg. Chem.*, 2018, 4393–4412.
- 20 C. J. Weiss, E. S. Wiedner, J. A. Roberts and A. M. Appel, *Chem. Commun.*, 2015, **51**, 6172–6174.
- 21 T. Gunasekara, Y. Tong, A. L. Speelman, J. D. Erickson, A. M. Appel, M. B. Hall and E. S. Wiedner, *ACS Catal.*, 2022, **12**, 2729–2740.
- 22 S. P. Heins, P. E. Schneider, A. L. Speelman, S. Hammes-Schiffer and A. M. Appel, *ACS Catal.*, 2021, **11**, 6384–6389.
- 23 E. A. McLoughlin, B. D. Matson, R. Sarangi and R. M. Waymouth, *Inorg. Chem.*, 2020, **59**, 1453–1460.
- 24 C. M. Galvin and R. M. Waymouth, *J. Am. Chem. Soc.*, 2020, **142**, 19368–19378.
- 25 K. M. Waldie, K. R. Flajlslik, E. McLoughlin, C. E. Chidsey and R. M. Waymouth, *J. Am. Chem. Soc.*, 2017, **139**, 738–748.
- 26 E. A. McLoughlin, K. C. Armstrong and R. M. Waymouth, *ACS Catal.*, 2020, **10**, 11654–11662.
- 27 A. Badalyan and S. S. Stahl, *Nature*, 2016, **535**, 406–410.
- 28 E. J. Nurminen, J. K. Mattinen and H. Lönnberg, *J. Chem. Soc., Perkin Trans. 2*, 2001, 2159–2165.
- 29 S. Horvath, L. E. Fernandez, A. V. Soudackov and S. Hammes-Schiffer, *Proc. Natl. Acad. Sci. U. S. A.*, 2012, **109**, 15663–15668.
- 30 L. E. Fernandez, S. Horvath and S. Hammes-Schiffer, *J. Phys. Chem. C*, 2012, **116**, 3171–3180.
- 31 C. J. Curtis, A. Miedaner, R. Ciancanelli, W. W. Ellis, B. C. Noll, M. Rakowski DuBois and D. L. DuBois, *Inorg. Chem.*, 2003, **42**, 216–227.
- 32 W. Baratta, G. Chelucci, S. Gladiali, K. Siega, M. Toniutti, M. Zanette, E. Zangrando and P. Rigo, *Angew. Chem., Int. Ed.*, 2005, **44**, 6214–6219.
- 33 P. J. Bonitatibus, Jr., S. Chakraborty, M. D. Doherty, O. Siclován, W. D. Jones and G. L. Soloveichik, *Proc. Natl. Acad. Sci. U. S. A.*, 2015, **112**, 1687–1692.
- 34 S. Chakraborty, P. O. Lagaditis, M. Förster, E. A. Bielinski, N. Hazari, M. C. Holthausen, W. D. Jones and S. Schneider, *ACS Catal.*, 2014, **4**, 3994–4003.
- 35 Z. E. Clarke, P. T. Maragh, T. P. Dasgupta, D. G. Gusev, A. J. Lough and K. Abdur-Rashid, *Organometallics*, 2006, **25**, 4113–4117.
- 36 F. Wang and S. S. Stahl, *Acc. Chem. Res.*, 2020, **53**, 561–574.
- 37 J. E. Nutting, M. Rafiee and S. S. Stahl, *Chem. Rev.*, 2018, **118**, 4834–4885.
- 38 B. J. Taitt, M. T. Bender and K.-S. Choi, *ACS Catal.*, 2020, **10**, 265–275.
- 39 B. L. Ryland and S. S. Stahl, *Angew. Chem., Int. Ed.*, 2014, **53**, 8824–8838.
- 40 D. P. Hickey, D. A. Schiedler, I. Matanovic, P. V. Doan, P. Atanassov, S. D. Minter and M. S. Sigman, *J. Am. Chem. Soc.*, 2015, **137**, 16179–16186.
- 41 C.-M. Che and W.-O. Lee, *J. Chem. Soc., Chem. Commun.*, 1988, 881–882.
- 42 H. Ozawa, T. Hino, H. Ohtsu, T. Wada and K. Tanaka, *Inorg. Chim. Acta*, 2011, **366**, 298–302.
- 43 C. Sens, M. Rodriguez, I. Romero, A. Llobet, T. Parella and J. Benet-Buchholz, *Inorg. Chem.*, 2003, **42**, 8385–8394.
- 44 X. Sala, A. Poater, I. Romero, M. Rodriguez, A. Llobet, X. Solans, T. Parella and T. M. Santos, *Eur. J. Inorg. Chem.*, 2004, 612–618.
- 45 M. Rodriguez, I. Romero, A. Llobet, A. Deronzier, M. Biner, T. Parella and H. Stoeckli-Evans, *Inorg. Chem.*, 2001, **40**, 4150–4156.
- 46 N. Chanda, B. Mondal, V. G. Puranik and G. K. Lahiri, *Polyhedron*, 2002, **21**, 2033–2043.
- 47 V. J. Catalano, R. A. Heck, C. E. Immoos, A. Ohman and M. G. Hill, *Inorg. Chem.*, 1998, **37**, 2150–2157.
- 48 K. R. Brownell, C. C. McCrory, C. E. Chidsey, R. H. Perry, R. N. Zare and R. M. Waymouth, *J. Am. Chem. Soc.*, 2013, **135**, 14299–14305.
- 49 S. Yamazaki, M. Yao, N. Fujiwara, Z. Siroma, K. Yasuda and T. Ioroi, *Chem. Commun.*, 2012, **48**, 4353–4355.
- 50 S. P. Annen, V. Bambagioni, M. Bevilacqua, J. Filippi, A. Marchionni, W. Oberhauser, H. Schonberg, F. Vizza, C. Bianchini and H. Grützmacher, *Angew. Chem., Int. Ed.*, 2010, **49**, 7229–7233.
- 51 M. Bevilacqua, C. Bianchini, A. Marchionni, J. Filippi, A. Lavacchi, H. Miller, W. Oberhauser, F. Vizza, G. Granozzi, L. Artiglia, S. P. Annen, F. Krumeich and H. Grützmacher, *Energy Environ. Sci.*, 2012, **5**, 8608–8620.



- 52 S. Najafshirtari, K. Friedel Ortega, M. Douthwaite, S. Pattison, G. J. Hutchings, C. J. Bondue, K. Tschulik, D. Waffel, B. Peng, M. Deitermann, G. W. Busser, M. Muhler and M. Behrens, *Chem. – Eur. J.*, 2021, **27**, 16809–16833.
- 53 H. Lei, P. Atanassova, Y. Sun and B. Blizanac, State-of-the-Art Electrocatalysts for Direct Methanol Fuel Cells, in *Electrocatalysis of Direct Methanol Fuel Cells*, ed. H. Liu and J. Zhang, Wiley-VCH Verlag GmbH & Co. KGaA, Weinheim, 2009, ch. 5, pp. 197–226.
- 54 S. L. Blair and W. L. Law, Electrocatalysis in Other Direct Liquid Fuel Cells, in *Electrocatalysis of Direct Methanol Fuel Cells*, ed. H. Liu and J. Zhang, Wiley-VCH Verlag GmbH & Co. KGaA, Weinheim, 2009, pp. 527–566.
- 55 N. Kakati, J. Maiti, S. H. Lee, S. H. Jee, B. Viswanathan and Y. S. Yoon, *Chem. Rev.*, 2014, **114**, 12397–12429.
- 56 H. Huang, C. Yu, X. Han, H. Huang, Q. Wei, W. Guo, Z. Wang and J. Qiu, *Energy Environ. Sci.*, 2020, **13**, 4990–4999.
- 57 M. T. Bender, Y. C. Lam, S. Hammes-Schiffer and K. S. Choi, *J. Am. Chem. Soc.*, 2020, **142**, 21538–21547.
- 58 W.-J. Liu, L. Dang, Z. Xu, H.-Q. Yu, S. Jin and G. W. Huber, *ACS Catal.*, 2018, **8**, 5533–5541.
- 59 M. T. Bender, X. Yuan and K. S. Choi, *Nat. Commun.*, 2020, **11**, 4594.
- 60 In other work (ref. 10), solvation free energies have been estimated computationally. This approach required benchmarking, and still resulted in uncertainty on the order of 1–2 kcal mol<sup>-1</sup>. For alcohol oxidation, computationally estimated values are therefore unlikely to provide a substantial improvement in accuracy compared to neglecting solvation free energies.

